

Channeling study on damage in potassium titanyl phosphate induced by ion irradiation

Ke-Ming Wang, Bo-Rong Shi, Zhong-Lie Wang, and Xiang-Dong Liu
Department of Physics, Shandong University, Jinan 250100, Shandong, China

Yao-Gang Liu
Institute of Crystal Material, Shandong University, Jinan 250100, Shandong, China

Qing-Tai Zhao
Department of Physics, Peking University, Beijing 100871, China
(Received 15 March 1994)

Potassium titanyl phosphate (KTiOPO₄ or KTP) is a quadriatomic material made of O, P, K, and Ti which crystallizes in an orthorhombic structure with space group *Pna*2. The virgin KTP at different axial orientation, $\langle 100 \rangle$, $\langle 001 \rangle$, and $\langle 010 \rangle$, has been investigated by the channeling technique. The obtained corresponding minimum yields are 3.8, 4, and 11 %, respectively. Damage in KTP was created by 200 and 400 keV He-, Xe-, and Hg-ion irradiations with the dose varying from 1×10^{13} to 1×10^{16} ions/cm². The effect of ion mass, energy, dose, annealing temperature, and orientation of KTP on the damage has been studied. The number of displaced atoms, the damage peak, and damage width are extracted from the experimental data. The numbers of the displaced atoms obtained are compared with the TRIM code (the transport of ions in the matters). The result shows that the experimental numbers of the displaced atoms are in agreement with theoretical ones predicted by the TRIM code within the order of the magnitude. Also for the case of He ion implanted in KTP to a dose of 1×10^{16} ions/cm², the recovery of the crystallinity of the KTP is observed after 800°C annealing.

I. INTRODUCTION

Potassium titanyl phosphate (KTiOPO₄ or KTP) is a relatively new and attractive material with applications in electro-optics.¹⁻³ It is used in the frequency doubling of near-infrared lasers and has been employed to produce a Mach-Zehnder electro-optics wave-guide device capable of modulating light at up to 12 GHz.⁴ The large non-linear optical coefficient combined with a high optical damage threshold make this material presently one of the most useful for nonlinear optical devices and integrated optical application.^{5,6}

The use of ion implantation to change the physical property, for example, the refractive index, of KTP may be interesting. In 1992, Zhang and co-workers reported the ion-implanted optical wave guide in the nonlinear material KTP and second-harmonic generation in an ion-implanted KTP wave guide.^{7,8} A major effect of ion irradiation in optoelectrical materials is the modification of the refractive index.⁹ The change of the refractive index depends on the radiation damage produced by ion implantation. Accurate information of the damage profile created by ion irradiation is important for a variety of reasons. In the ion-implantation technique, it has been found that the annealing behavior depends on the character and intensity of the damage.¹⁰ In order to understand and predict the results of implantation and annealing processes, we need to know the damage distribution.

Channeling has been shown to be a powerful tool in the study of radiation damage created from ion irradiation in crystal.¹¹ The channeling technique yields not only the

amount of damage, but also contains parameters of the depth distribution of the damage. Because of extra dechanneling from the displaced atoms, the damage profile is not simply given by the difference of the two spectra; the yield in the post-implant spectrum is a sum of direct scattering of channeled ions from the damage centers and scattering from the nonchanneled part of the beam. To determine the depth distribution of the damage from these spectra, the dechanneling must be considered.

To our knowledge, previous ion-channeling studies in KTP have not been reported. The main purposes of this work are first, to give measurement results of random and aligned spectra for virgin KTP in different orientations; second, to present the damage dependence on ion mass, energy, dose, annealing, and orientation of KTP; third, to extract the damage peak, damage width and number of the displaced atoms from present experimental data as well as to compare the number of the displaced atoms extracted with the TRIM code (the transport of ions in the matters).

II. EXPERIMENT

A. Sample preparation

The potassium titanyl phosphate (KTP) crystal used in this work was provided by the Institute of Crystal Material, Shandong University. Before cutting, the quality of KTP crystal was checked using Rutherford back-scattering. Samples 1 mm thick were cut along three sets of planes: (100), (010), and (001) from a large KTP crys-

tal. The direction of the sample was investigated using x-ray diffraction. The samples were optically polished and cleaned before irradiation.

B. Damage production

The damage in KTP was produced by ion irradiation. The ion irradiations were performed using a 400-kV ion implanter at Shandong University. In order to ensure uniformity over the implanted area, a two-directional electrostatic scanning system was used. The system for parallel scanning of the beam consisted of four sets of deflection plates. A neutral beam trap was also employed. The irradiations were carried out at room temperature. Different ions were chosen such as He^+ , Xe^+ , and Hg^+ with energies varying from 200 keV to 400 keV. The implantation doses in range from 1×10^{13} and 1×10^{16} ions/cm² were employed for He, Xe, and Hg ions, respectively. The integration of the ion current to the target was used to achieve highly accurate dose measurement. In order to study the damage dependence on the orientation of KTP crystal, the samples which have been cut in different orientation were irradiated by ions in the same condition.

C. Thermal annealing

In order to investigate the thermal annealing behavior of damage in KTP induced by ion irradiation, a set of samples which were cut along (100) plane were chosen. The samples were irradiated by 400-keV He ion with a dose of 1×10^{16} ions/cm², and then annealed at various temperatures.

D. Rutherford backscattering channeling measurement

The KTP samples were analyzed by the Rutherford backscattering (RBS) and channeling technique with 2.1-MeV $^4\text{He}^{2+}$ from 2×1.7 -MV tandem accelerator of Shandong University. The samples were mounted in a three-dimensional goniometer that had an accuracy of 0.01°. The target rotation was controlled by stepping motors that were controlled by a computerized system, which also determined the alignment corresponding to the minimum of the backscattering particles. The backscattered particles were detected at a scattering angle of 165° with a surface barrier detector. The probed area was 1 mm² in size and the He beam current typically is 10 nA. The amplified pulses from the detector were transferred to a multichannel analyzer and the spectra were finally stored in a computer for data analysis. The ion beam was collimated with two slits which can be adjusted in the experiment. The energy resolution of the solid-state detector is 18 keV. The angle of collimation of the ion beam is less than 0.001°.

III. RESULTS

Potassium titanyl phosphate (KTP) is a quadriatomic material made of O, P, K, and Ti. KTP crystallizes in an orthorhombic structure with space group *Pna*2. Lattice constants are $a = 12.814$ Å, $b = 10.61$ Å, and $c = 6.404$

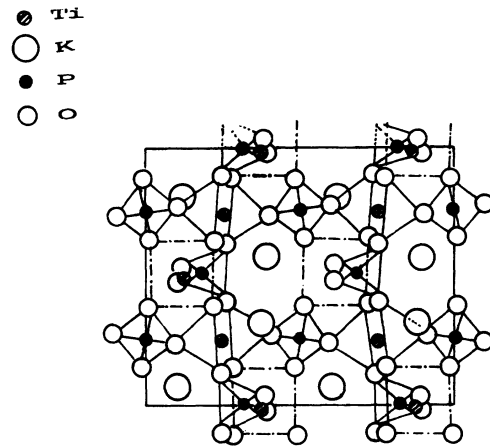


FIG. 1. Projection of the normal KTP[001] structure.

Å. This compound is a monophosphate. Each atom of the asymmetric unit is replicated in four sites by the symmetry operations of the space group. KTP contains two different types of titanium sites, denoted Ti1 and Ti2. Each titanium atom in the normal structure is coordinated to six oxygen atoms. Four of these belong to phosphate groups, while the other two, denoted chain oxygens, are involved in an infinite chain of alternating titanium and oxygen atoms. One difference between Ti1 and Ti2 is that the two chain oxygens coordinated to Ti1 make a bond angle O-Ti1-O of roughly 90°, while the two chain oxygens coordinated to Ti2 make an angle O-Ti2-O of 180°.¹² Figure 1 shows a projection of the KTP[001] structure.¹³ The corresponding axial channeling spectrum and random spectrum are given in Fig. 2 for virgin KTP. From Fig. 2 the minimum yield is 4%. Figure 3 depicts the projection of KTP[010] structure. Random spectrum of virgin KTP crystal and aligned spectrum of KTP<010> axial direction are shown in Fig. 4. The random spectra were obtained by rotating while tilted away

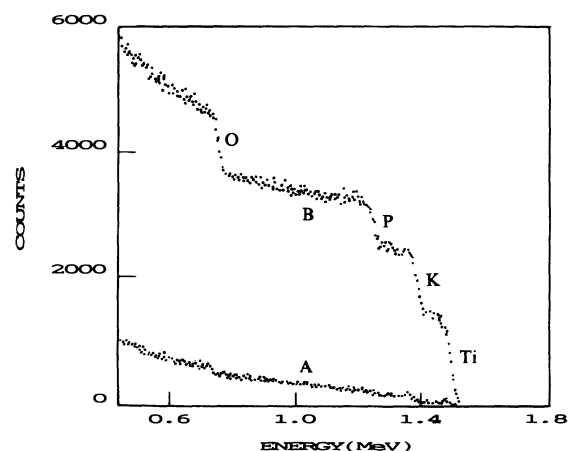


FIG. 2. RBS/channeling spectra. The minimum yield is 4%. (A) Channeling spectrum for 2.1-MeV He ions incident in the <001> axial direction of a virgin KTP. (B) Random spectrum of KTP.

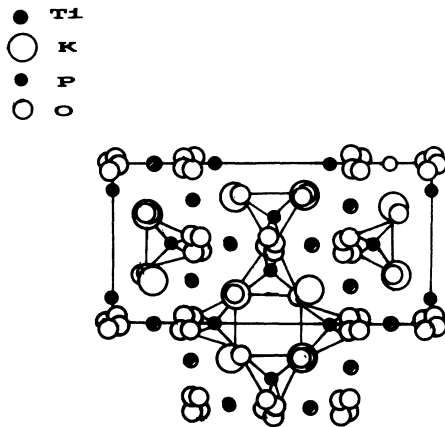


FIG. 3. Projection of the normal KTP[010] structure.

from a channeling direction. The minimum yield is 11%. In order to observe the effect of the crystal orientation on the minimum yield, $\langle 100 \rangle$ axial direction is also chosen. For KTP $\langle 100 \rangle$ axial direction the minimum yield is 3.8%. In this work, the minimum yield is defined as the ratio of the height of valley of Ti surface peak to one of corresponding random spectrum. Ideally, this should be performed at the same depth of penetration of the ion beam.

The He backscattering spectra are recorded for the channeling and nonchanneling direction. The difference in the normalized yield curves (defined as the channeling spectrum divided, point by point, by the nonchanneling spectrum) for pre- and post-implant conditions was taken as a measure of the damage caused by the irradiation.

A. Mass dependence

The effect of ion mass on the induced radiation damage was observed by implanting 400-keV ^{202}Hg and ^{132}Xe

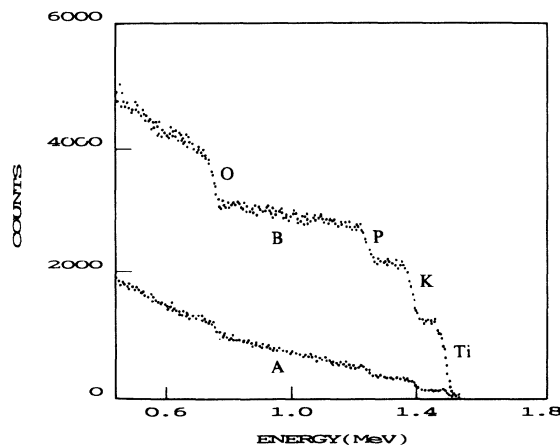


FIG. 4. RBS/channeling spectra. The minimum yield is 11%. (A) Channeling spectrum for 2.1-MeV He ions incident in the $\langle 010 \rangle$ axial direction of a virgin KTP. (b) Random spectrum of KTP.

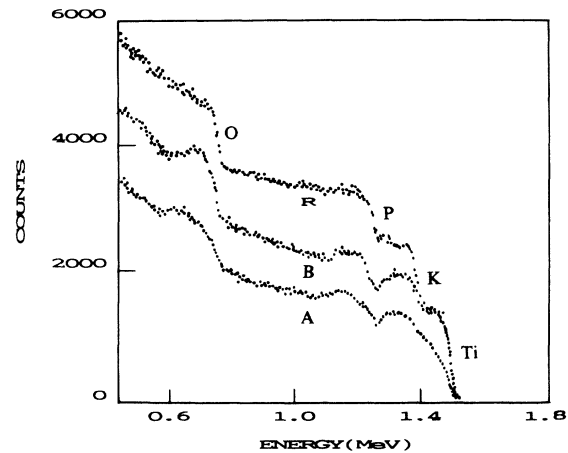


FIG. 5. Channeling spectra in the $\langle 010 \rangle$ axial direction of KTP irradiated by 400-keV Hg ions and 400-keV Xe ions with a dose of 1×10^{13} ions/cm². (A) 400-keV Xe ions; (B) 400-keV Hg ions. *R* represents random spectrum of KTP.

ions to a dose of 1.0×10^{13} ions/cm² into a $\langle 010 \rangle$ KTP crystal. The results are shown in Fig. 5. Figure 5 shows that for the lighter ion implant, the damage peak occurs at a lower energy on the backscattering spectrum and thus indicates that the damage peak is at a greater depth into the KTP crystal as expected. The height of the damage peak created by Hg ions is higher than the one created by Xe ion. The damage width created by Hg ion is narrower than one created by Xe ions. It is concluded that the damage in KTP depends strongly on the ion mass for the cases of both Hg⁺ and Xe⁺ irradiations. The ratio of their damage widths corresponds approximately to that of their range stragglings, as discussed subsequently.

B. Energy dependence

In order to see the effect of ion energy on the damage, we have used Hg ion implanted at room temperature in a $\langle 010 \rangle$ KTP crystal. The energy was chosen at 200 and 400 keV with the same dose of 1×10^{13} ions/cm². The random and aligned spectra are shown in Fig. 6. From Fig. 6, it is observed that the position of the damage peak produced by 400-keV Hg ion is deeper than one produced by 200-keV Hg ion. The ratio of widths of the damage distribution is 1.73. According to our measurement result of Hg ions in amorphous KTP, the range stragglings obtained for 400- and 200-keV Hg ions in KTP are 348 Å and 231 Å, respectively. Hence, the ratio of the range stragglings is closer to the ratio of the damage distribution.

C. Dose dependence

For comparing the dose dependence of damage created at room temperature by Xe ion in KTP, we used two KTP samples which were cut along the $\langle 001 \rangle$ plane. There was no special purpose for choosing this orientation. The irradiation doses were 1×10^{13} and 5×10^{13}

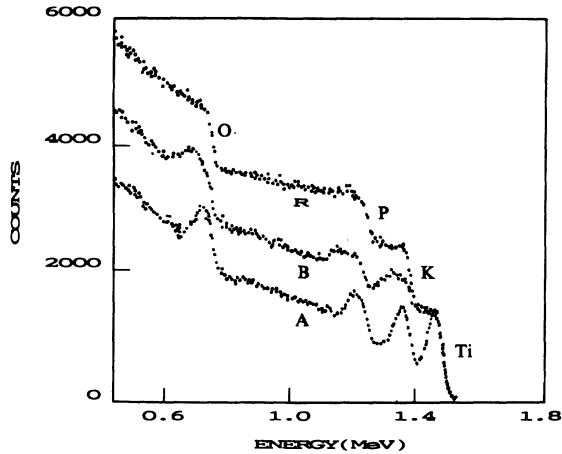


FIG. 6. Channeling spectra in the $\langle 010 \rangle$ axial direction of KTP irradiated by Hg ions with a dose of 1×10^{13} at 200 keV and 400 keV, but the current density is different. (A) 200-keV Hg ions; (B) 400-keV Hg ions. R represents random spectrum of KTP.

ions/cm² and the energy was 200 keV. As shown in Fig. 7, the amount of damage increases with the dose. The ratio of amplitude of the damage is 1.26 for the dose of 5×10^{13} ions/cm² and 1×10^{13} ions/cm². From Fig. 7 it is observed that the saturation of the damage is not approached for the case of the dose 5×10^{13} ions/cm² for Xe ions implanted in KTP.

D. Annealing behavior

A $\langle 100 \rangle$ KTP sample was irradiated with 400-keV He ion to a dose of 1×10^{16} ions/cm² and then annealed at 200, 400, 600, and 800 °C in oxygen atmosphere. The channeled spectra in post annealing are shown in Fig. 8 where we can see that with increasing of annealing temperature, the number of displaced atoms is decreased. After a 5-min annealing at 800 °C, the minimum yield is

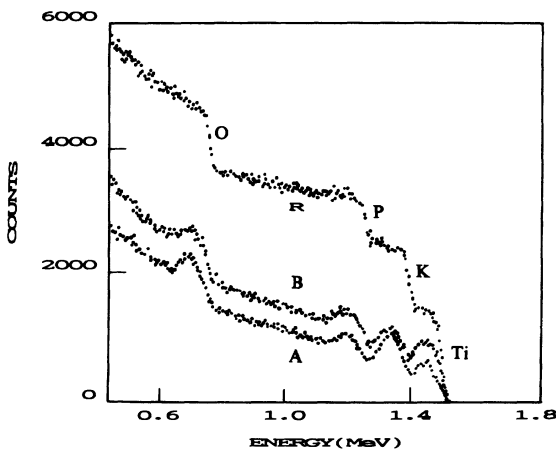


FIG. 7. Channeling spectrum in the $\langle 001 \rangle$ axial direction of KTP irradiated by 200-keV Xe ions with the dose of 1×10^{13} ions/cm² and 5×10^{13} ions/cm². (A) 1×10^{13} ions/cm²; (B) 5×10^{13} ions/cm². R represents random spectrum of KTP.

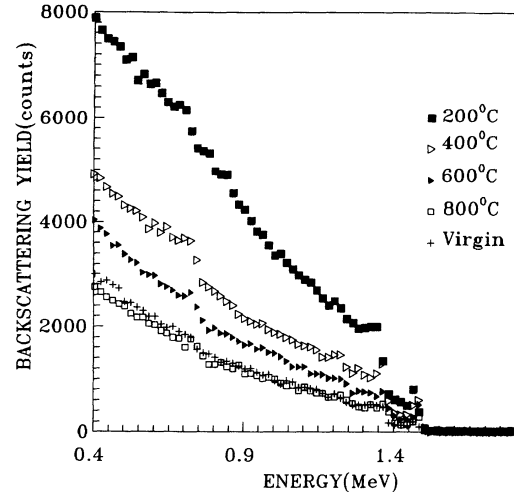


FIG. 8. Channeled spectra in the axial direction $\langle 100 \rangle$ of KTP irradiated by 400-keV He ions to a dose of 1×10^{16} ions/cm² in different annealing temperature.

3.6% which is closer to 3.8% of virgin KTP. This fact indicates the recovery of crystallinity of KTP.

E. Orientation dependence

To observe the effect of the orientation of KTP on the damage during the ion irradiation, we have used two samples which were cut along $\langle 100 \rangle$ and $\langle 001 \rangle$ planes. The KTP samples were irradiated by 200-keV Xe⁺ with the same dose of 1×10^{13} ions/cm². Figure 9 represents the comparison between aligned spectra for KTP $\langle 100 \rangle$ and $\langle 001 \rangle$ axial direction. The backscattering yield obtained for $\langle 100 \rangle$ axial direction is higher than one for $\langle 001 \rangle$ axial direction. This result may be explained as two reasons. First is that the ion-induced damage probably depends on the orientation of the KTP. Second is that the dechanneling fraction is different due to arrangement of the atom in the two different channels.

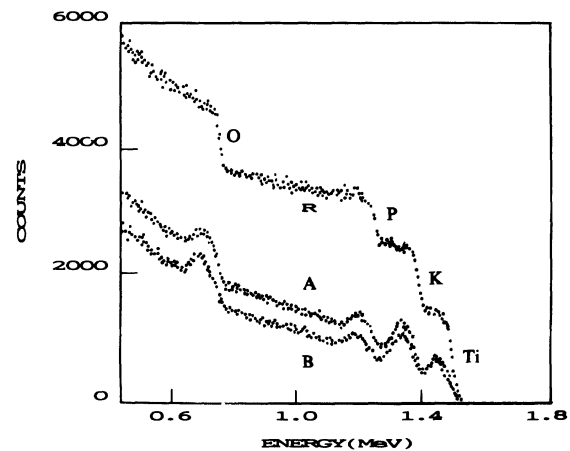


FIG. 9. Channeled spectra for KTP irradiated by 200-keV Xe ions with a dose of 1×10^{13} ions/cm² at different orientation. (A) $\langle 100 \rangle$ axial direction; (B) $\langle 001 \rangle$ axial direction. R represents random spectrum of KTP.

IV. DATA ANALYSIS AND DISCUSSION

The damage profiles created by ion implantation in solids have been studied quite extensively, particularly in a monatomic crystal like Si.¹⁴⁻¹⁶ Atomic collision cascade theory has been developed to predict the damage profile in a variety of cases. It is known that a theoretical treatment of damage profiles for ion in polyatomic target is complicated. Götz suggests¹⁷ that the mean damage range R_d and the damage range straggling ΔR_d created by ion irradiation can be replaced by the mean projected range R_p and the range straggling ΔR_p of ions implanted in solids in a fairly good approximation. But in general the damage profile legs the implant profile and the damage profile is broader than the range profile for Si.

A. Calculation of range profile parameter

In general, the implanted ion distribution can be described by Pearson distribution of type IV using the four moments projected range, range straggling (standard deviation), skewness, and kurtosis.¹⁸ It is well known that Lindhard, Sharff, and Shiøtt (LSS) theory is widely used for calculation of low velocity ion ranges in solids, originally developed for a monatomic target.¹⁹ Although Gibbons, Johnson, and Mylroie used the LSS procedure to calculate the mean projected range and range straggling of ions in polyatomic target, the target is limited to three elements or less.²⁰ The Monte Carlo simulation can be employed for calculating the mean projected range and range straggling as well as other parameters of ions in the polyatomic target made of four elements or less.²¹ KTP is a four-element target made of O, P, K, and Ti. We have developed a method to calculate the mean projected range and range straggling of heavy ions in polyatomic target based on Biersack's angular diffusion model.^{22,23} The calculation procedure is given in detail elsewhere.²⁴ Table I summarizes the data on the mean projected range and range straggling of He⁺, Xe⁺, and Hg⁺ in amorphized KTP obtained by TRIM'89 code and our calculation procedure. Experimental mean projected range and range straggling is higher than calculated ones. The reason is not known. This phenomenon is similar to the result reported in Refs. 25 where Grande and co-workers have studied the range profiles of heavy ions in C film and found a large difference between the experimental values and the prediction of Ziegler, Biersack, and Littmark,

with theory predicting the mean projected range being about 45% of the experimental value. As for the range straggling, the experimental values always exceed the predicted ones, the difference being almost 100%. But they found that good agreement is achieved only after inelastic effects are included in nuclear stopping power regime for Au and Bi implanted into photoresist films.²⁶

B. Extraction of parameters of damage distribution

It is difficult to calculate the parameters of damage distribution created by ions in such polyatomic target as KTP. We can ask what quantitative information may be obtained from present experimental data. This is our data in using characteristic atom O in KTP for getting such information. The following assumptions are made: (1) The quadriatomic target KTP is equivalent to a "mean element target" with an atomic number equal to the average atomic number of KTP and a mass equal to the average atomic mass of the KTP. (2) Ratio of stopping power of channeled to random direction for He ion in O, P, K, and Ti of KTP is 0.5. We have then used the procedure by Feldman and Rodgers to estimate the damage distribution parameters.²⁷

1. Damage peak and width

The energy of a particle $E_d(t)$ with incident energy E_1 , which remains in the channel for a depth t , then scatters to an angle $(\pi-\theta)$ and emerges in a nonchanneling direction is given by

$$E_d(t) = E_1 - t(dE/dX)_1 - K_1[E_1 - t(dE/dX)_1] - (1/\cos\theta)(dE/dX)_2, \quad (1)$$

where $(dE/dX)_1$ is the stopping power for particle entering in the channel, $(dE/dX)_2$ is the stopping power for the emerging particle. The third term represents the kinematic energy loss due to actual collision of the He ions of energy $[E_1 - t(dE/dX)_1]$ with a target atom. This equation may be solved for t to give

$$t = [E_a - E_d(t)] / [(1 - k_1)(dE/dX)_1 + (dE/dX)_2 / \cos\theta], \quad (2)$$

where $E_a = E_1 - K_1 E_1 = K E_1$ and is the energy of a parti-

TABLE I. Projected range R_p and range straggling ΔR_p of He⁺, Xe⁺, and Hg⁺ in amorphous KTP used for damage production. Experimental data of projected range and range straggling of Xe⁺ and Hg⁺ in KTP crystal come from Refs. 32 and 33.

Ion	Energy (keV)	Projected range R_p (Å)			Range straggling ΔR_p (Å)		
		TRIM'89	Our calc.	Expt.	TRIM'89	Our calc.	Expt.
He	400	14 000			1400		
Xe	200	654	727	862	172	179	284
Xe	400	1 134	1326	1693	288	300	491
Hg	200	586	641	754	135	135	231
Hg	400	985	1039	1339	226	205	348

TABLE II. The experimental values of the total displaced O atoms, damage peak, and damage width created by 200-keV Hg, 400-keV Hg, and 400-keV Xe ions with a dose of 1×10^{13} ions/cm². The theoretical values of the total displaced O atoms are obtained by TRIM code.

Ion	Energy (keV)	Total displaced O atoms (10^{16} cm ⁻²)		Damage peak (Å)	Damage width (Å)
		Expt.	TRIM		
Hg	200	5.59	4.79	856	436
Hg	400	8.19	8.59	1478	756
Xe	400	2.90	7.24	1711	877

cle scattered from the surface. K is the kinematic factor. Thus the depth of the peak of the damage is simply proportional to the energy difference of the surface peak and the damage peak. The damage width can be estimated from the above equations also.

2. Total displaced atoms

Due to the extra dechanneling from the displaced atoms the damage profile is not simply given by the difference of the two spectra, but at any energy or depth, the yield in post implant spectrum is a sum of direct scattering of channeled ions from the damage centers and scattering from the nonchanneled part of the beam.²⁸⁻³¹ Therefore to determine the depth distribution of the damage from these spectra, the dechanneling must be considered. The displaced atoms can increase the measured yield of a damaged KTP crystal in two ways: (1) by deflecting the particles out of the channel so they become part of the normal beam and then available to scatter, i.e., dechanneling; (2) by direct scattering of the channeled beam from the displaced atoms. Both displaced particles and the ones in regular sites can deflect the incident beam out of the channel. Over most of the range of defect densities, the multiple scattering is the dominant dechanneling mechanism. However, only for some very low-damage cases single scattering may dominate and each individual case must be decided separately. The disorder distribution is simply given by

$$N_d(t)/N = [X_2(t) - f_n(t)] / [1 - f_n(t)], \quad (3)$$

where $N_d(t)$ and N are displaced atoms and host atoms in unit volume at depth t , respectively. X_2 is the normalized yield from a damaged crystal at any depth t and $f_n(t)$ is the fraction of the beam normal at depth t . $f_n(t)$ may be estimated under two different assumptions of the dechanneling mechanisms: single scattering and multiple scattering. For multiple scattering,

$$f_n(t) = X_1(t) + [1 - X_1(t)] \exp[-\psi_c^2 / \Omega^2(t)], \quad (4)$$

where $X_1(t)$ is the perfect crystal yield at depth t ,

$$\Omega^2(t) = (\pi/2) \psi_1^4 d^2 L_n \int_0^t N_d(t') dt', \quad (5)$$

where $\psi_1 = (2Z_1 Z_2 e^2 / Ed)^{1/2}$ and $L_n = \ln(1.29\epsilon)$. ψ_c is the critical angle for channeling.

We can see that all quantities in the equations are known experimentally or may be estimated and thus $N_d(t)$ may be calculated by an iterative procedure. Table II shows the experimental values of total displacement O atoms, damage peak, and damage width created by Xe and Hg ions in KTP. From Table I and Table II, it is found that the damage peak is closer to the projected range and the damage profile is broader than the range profile. In order to compare the experimental value with the theoretical one on the number of displaced atoms, we have used the TRIM code to calculate it. The results are listed in Table II.

V. SUMMARY

Potassium titanyl phosphate (KTiOPO₄ or KTP crystal) is a quadriatomic material made of O, P, K, and Ti in an orthorhombic structure with space group $Pna2$. This is the first time we have used the Rutherford backscattering and channeling technique to study the virgin KTP at different orientations and the damage in KTP crystal created by ion irradiation. The minimum yields obtained were 3.8, 4, and 11 % for virgin KTP at $\langle 100 \rangle$, $\langle 001 \rangle$, and $\langle 010 \rangle$ axial directions, respectively. These values are closer to one of a silicon crystal. This is an indication of the degree of KTP crystal perfection. The damage peak is closer to the projected range and the damage profile is broader than range profile for both Hg and Xe implanted in KTP. The ratio of damage width to damage peak is about 0.5. This result is similar with one reported by Feldman and Rodgers for Si. For the case of 400-keV He⁺ implanted in KTP to a dose of 1×10^{16} ions/cm², the recovery of crystallinity of KTP is observed after 800°C annealing for 5 min. The present results show that the numbers of displaced O atoms induced by 200-keV Hg, 400-keV Hg, and 400-keV Xe ions in KTP are in agreement with ones predicted by TRIM code within the order of magnitude. It seems reasonable that the recombination is not important for the case of KTP induced by heavy ions such as Xe and Hg in low dose irradiation.

ACKNOWLEDGMENTS

The authors would like to thank Liu Ji-Tian and Lu Ju-Xin for their help in this work. This work was supported by National Natural Science Foundation of China.

- ¹J. D. Bierlein and C. B. Arweiler, *Appl. Phys. Lett.* **49**, 917 (1986).
- ²F. C. Zumsteg, J. D. Bierlein, and T. E. Gier, *J. Appl. Phys.* **47**, 4980 (1976).
- ³D. B. Laubacher, V. Guerra, M. P. Chouinard, J. Y. Liou, and P. H. Wyant, *Proc. Soc. Photo-Opt. Instrum. Eng.* **993**, 80 (1988).
- ⁴T. A. Driscoll, H. J. Hoffman, R. E. Stone, and P. E. Perkins, *J. Opt. Soc. Am. B* **3**, 683 (1986).
- ⁵J. D. Bierlein, A. Ferretti, L. H. Brixner, and W. Y. Hsu, *Appl. Phys. Lett.* **50**, 1216 (1987).
- ⁶W. P. Risk, *Appl. Phys. Lett.* **58**, 19 (1991).
- ⁷L. Zhang, P. J. Chandler, P. D. Townsend, and P. A. Thomas, *Electron. Lett.* **28**, 650 (1992).
- ⁸L. Zhang, P. J. Chandler, P. D. Townsend, Z. T. Alwahabi, and A. J. McCaffery, *Electron. Lett.* **28**, 1478 (1992).
- ⁹P. D. Townsend, *Nucl. Instrum. Methods Phys. Res. Sect. B* **46**, 18 (1990).
- ¹⁰J. Narayan, O. S. Oen, and S. J. Pennycook, in *Frontiers in Electronic Materials and Processing*, Proceedings of the First Topical Conference on Frontiers in Electronic Materials and Processing, edited by L. J. Brillson, AIP Conf. Proc. No. 138 (AIP, New York, 1986), p. 122.
- ¹¹L. C. Feldman, J. W. Mayer, and S. T. Picraux, *Materials Analysis by Ion Channeling* (Academic, New York, 1982).
- ¹²M. G. Roelofs, *J. Appl. Phys.* **65**, 4976 (1989).
- ¹³I. Tordjman, R. Masse, and J. C. Guitel, *Z. Kristallogr.* **139**, 103 (1974).
- ¹⁴J. A. Davies, J. Denhartog, L. Eriksson, and J. W. Mayer, *Can. J. Phys.* **45**, 4053 (1967).
- ¹⁵J. W. Mayer, L. Eriksson, S. T. Picraux, and J. A. Davies, *Can. J. Phys.* **46**, 663 (1968).
- ¹⁶J. Linnros, G. Holmen, and B. Svensson, *Phys. Rev. B* **32**, 2770 (1985).
- ¹⁷G. Götz, in *Ion Beam Modification of Insulators*, edited by P. Mazzoldi and G. W. Arnold (Elsevier, New York, 1987), p. 412.
- ¹⁸H. Ryssel, K. Habegger, K. Hoffmann, G. Prinke, R. Dumcke, and A. Sachs, *IEEE Trans. Electron Devices* **27**, 1484 (1980).
- ¹⁹J. Lindhard, M. Scharff, and H. E. Schiøtt, *K. Dan. Vidensk. Mad. Fys. Medd.* **33**, 14 (1963).
- ²⁰J. P. Gibbons, W. S. Johnson, and S. W. Mylroie, *Projected Range Statistics* (Stroudsburg, Chicago, 1975).
- ²¹J. P. Biersack and L. G. Haggmark, *Nucl. Instrum. Methods* **174**, 257 (1980).
- ²²J. P. Biersack, *Nucl. Instrum. Methods* **182/183**, 199 (1981).
- ²³J. P. Biersack, *Z. Phys. A* **305**, 95 (1982).
- ²⁴Ke-Ming Wang and Bo-Rong Shi, *J. Phys. D* **23**, 1282 (1990).
- ²⁵P. L. Grande, P. F. P. Fichtner, M. Behar, and F. C. Zawislak, *Nucl. Instrum. Methods Phys. Res. Sect. B* **33**, 122 (1988).
- ²⁶M. Behar, P. L. Grande, L. Amaral, J. R. Kaschny, F. C. Zawislak, R. B. Guimarães, J. P. Biersack, and D. Fink, *Phys. Rev. B* **41**, 6145 (1990).
- ²⁷L. C. Feldman and J. W. Rodgers, *J. Appl. Phys.* **41**, 3776 (1970).
- ²⁸J. A. Ellison, S. T. Picraux, W. R. Allen, and W. K. Chu, *Phys. Rev. B* **37**, 7290 (1988).
- ²⁹S. T. Picraux, R. M. Biefeld, W. R. Allen, W. K. Chu, and J. A. Ellison, *Phys. Rev. B* **39**, 11 086 (1988).
- ³⁰E. Bøgh, *Can. J. Phys.* **46**, 653 (1968).
- ³¹J. Linnros, B. Svensson, and G. Holmen, *Phys. Rev. B* **30**, 3629 (1984).
- ³²Ke-Ming Wang, Bo-Rong Shi, Zhong-Lie Wang, Qing-Tai Zhao, Xiang-Dong Liu, and Yao-Gang Liu, *J. Appl. Phys.* **68**, 3975 (1990).
- ³³Ke-Ming Wang, Bo-Rong Shi, Zhong-Lie Wang, Qing-Tai Zhao, Yun-Tao Wang, Xiang-Dong Liu, and Ji-Tian Liu, *Phys. Lett. A* **151**, 241 (1990).